

Engagement of Collagen-Binding Integrins Promotes Matrix Metalloproteinase-9–Dependent E-Cadherin Ectodomain Shedding in Ovarian Carcinoma Cells

Jaime Symowicz,¹ Brian P. Adley,² Kara J. Gleason,¹ Jeffrey J. Johnson,¹ Supurna Ghosh,¹ David A. Fishman,³ Laurie G. Hudson,⁴ and M. Sharon Stack^{1,5}

Departments of ¹Cell and Molecular Biology and ²Pathology, Northwestern University Feinberg Medical School, Chicago, Illinois; ³Department of Obstetrics and Gynecology, New York University, New York, New York; ⁴Department of Pharmaceutical Sciences, College of Pharmacy, University of New Mexico, Albuquerque, New Mexico; and ⁵Robert H. Lurie Comprehensive Cancer Center, Northwestern University, Chicago, Illinois

Abstract

Reversible modulation of cell-cell adhesion, cell-matrix adhesion, and proteolytic activity plays a critical role in remodeling of the neoplastic ovarian epithelium during metastasis, implicating cadherins, integrins, and proteinases in i.p. metastatic dissemination of epithelial ovarian carcinoma (EOC). Aberrant epithelial differentiation is an early event in ovarian carcinogenesis; thus, in contrast to most carcinomas that lose E-cadherin expression with progression, E-cadherin is abundant in primary EOC. Metastasizing EOCs engage in integrin-mediated adhesion to submesothelial interstitial collagens and express matrix metalloproteinases (MMP) that facilitate collagen invasion, thereby anchoring secondary lesions in the submesothelial matrix. As metalloproteinases have also been implicated in E-cadherin ectodomain shedding, the current study was undertaken to model the effects of matrix-induced integrin clustering on proteinase-catalyzed E-cadherin ectodomain shedding. Aggregation of collagen-binding integrins induced shedding of an 80-kDa E-cadherin ectodomain [soluble E-cadherin (sE-cad)] in a MMP- and Src kinase-dependent manner, and sE-cad was prevalent in ascites from ovarian cancer patients. Expression of MMP-9 was elevated by integrin aggregation, integrin-mediated ectodomain shedding was inhibited by a MMP-9 function blocking antibody, and incubation of cells with exogenous MMP-9 catalyzed E-cadherin ectodomain shedding. In contrast to other tumors wherein sE-cad is released into the circulation, EOC tumors maintain direct contact with sE-cad-rich ascites at high concentration, and incubation of EOC cells with physiologically relevant concentrations of recombinant sE-cad disrupted adherens junctions. These data support a novel mechanism for posttranslational modification of E-cadherin function via MMP-9 induction initiated by cell-matrix contact and suggest a mechanism for promotion of EOC metastatic dissemination. [Cancer Res 2007;67(5):2030–9]

Introduction

Approximately 22,000 women are newly diagnosed with epithelial ovarian carcinoma (EOC) every year and 75% of these women present at diagnosis with disseminated i.p. metastases with

poor prognosis (1). Unlike other solid tumors, hematogenous dissemination of ovarian cancer cells rarely occurs, instead malignant ovarian epithelial cells exfoliate from the primary tumor as single cells or multicellular aggregates and attach at new sites throughout the peritoneal cavity. Disseminated cells also block the peritoneal lymphatics, contributing to the accumulation of malignant ascites (2, 3). The ascites is rich in growth factors, bioactive lipids, extracellular matrix (ECM) components, inflammatory mediators, and proteolytic enzymes (4–6), creating the unique ovarian cancer microenvironment that fosters further metastatic spread.

Reversible modulation of cell-cell adhesion, cell-matrix adhesion, and proteolytic activity plays a critical role in remodeling of the neoplastic ovarian epithelium during metastasis, implicating cadherins, integrins, and proteinases in i.p. dissemination. Whereas most epithelia express abundant E-cadherin, this cadherin is absent in the mesenchymally derived normal ovarian surface epithelia, which express neural cadherin. Aberrant epithelial differentiation is an early event in epithelial ovarian carcinogenesis, as tumors acquire increasingly complex differentiation reminiscent of the highly specialized epithelia of Mullerian duct origin (7). Thus, in contrast to most carcinomas that lose E-cadherin expression with progression, E-cadherin is abundant in primary differentiated EOCs and available data indicate a subsequent decrease of E-cadherin staining in peritoneal metastases (8–10). Whereas mutations in the *E-cadherin* gene are rare in ovarian carcinomas (11), post-translational modification of E-cadherin function is suggested by data showing soluble E-cadherin (sE-cad) in ascites and cystic fluids from ovarian cancer patients (12, 13).

Metastasizing EOCs adhere to peritoneal mesothelial cells and disrupt the mesothelial monolayer, exposing the type I/III collagen-rich submesothelial ECM. Ovarian carcinoma cells adhere to this exposed submesothelial ECM more strongly than to the mesothelial monolayer and exhibit preferential adhesion to interstitial collagen type I (3). Integrin engagement by an ECM ligand can result in receptor occupancy and/or aggregation, thus functionally coupling the extracellular environment to specific signal transduction pathways that modulate distinct cellular responses, including gene transcription, cell migration, and survival (14). Previous data from our laboratory and others have shown that proteinase expression and activity are regulated by integrin signaling, functionally coupling cell-matrix adhesion and proteinase-dependent invasion (15, 16). Proteolytic activity is important at multiple stages in i.p. metastasis to disrupt cell-cell contacts, facilitate invasion through the mesothelial layer, and anchor the secondary lesion in the submesothelial matrix. As metalloproteinases have been implicated

Requests for reprints: M. Sharon Stack, Department of Pathology and Anatomical Sciences, University of Missouri School of Medicine, One Hospital Dr., M263, Columbia, MO 65212. Phone: 573-884-7301; E-mail: Stackm@health.missouri.edu.

©2007 American Association for Cancer Research.
doi:10.1158/0008-5472.CAN-06-2808

in E-cadherin ectodomain shedding (17–21) and cell-matrix adhesion has been linked to matrix metalloproteinase (MMP) expression (15, 16), the current study was undertaken to evaluate a potential functional link between the interaction of cellular integrins with submesothelial interstitial collagens and decreased E-cadherin function. We report that aggregation of collagen-binding integrins promotes E-cadherin ectodomain shedding in a MMP and Src kinase-dependent manner. Integrin-mediated E-cadherin ectodomain shedding was reduced by a MMP-9 function blocking antibody and the shed ectodomain was generated on incubation of cells with exogenous active MMP-9. Furthermore, incubation of cells with physiologically relevant concentrations of recombinant E-cadherin ectodomain disrupted adherens junctions, suggesting that sE-cad at levels present in ovarian cancer ascites may play an active functional role in tumor dissemination. These studies provide a novel mechanism for post-translational modification of E-cadherin function induced by cell-matrix contact.

Materials and Methods

Materials. Mouse anti-E-cadherin (clone HECD-1) and mouse anti-E-cadherin (clone 4A2C7) were purchased from Invitrogen Corp. (Carlsbad, CA), formerly Zymed Laboratories, Inc. Mouse anti-human integrin β_1 (clone P5D2), mouse anti-human integrin α_3 (clone PIB5), and mouse anti-human integrin α_2 (clone P1E6) monoclonal antibodies, purified mouse IgG, and GM6001 were purchased from Chemicon International (Temecula, CA). Anti-MMP9 (Ab-1) mouse monoclonal antibody (6-6B) and PP2 in solution were purchased from Calbiochem (San Diego, CA). EZ-Link Sulfo-NHS-LC-Biotin and Ultralink Immobilized NeutrAvidin protein were purchased from Pierce (Rockford, IL). Protein G-Sepharose 4B FastFlow, recombinant protein G, cycloheximide in solution, and peroxidase-conjugated antimouse IgG were purchased from Sigma-Aldrich (St. Louis, MO). Purified recombinant MMP-9 was generously provided by Dr. Rafael Fridman (Wayne State University, Detroit, MI). It was activated by 1 mmol/L 4-aminophenylmercuric acetate (Sigma-Aldrich) and dialyzed in collagenase buffer [50 mmol/L Tris, 150 mmol/L NaCl, 5 mmol/L CaCl₂, 0.02% Brij-35 (pH 7.5)]. Alexa Fluor 488 goat anti-mouse IgG (H+L) was purchased from Molecular Probes (Eugene, OR).

Cell lines, ascites, and immunohistochemical analysis of human tumors. OVCA433 and OVCA429 cells were generously provided by Dr. Robert Bast (M. D. Anderson Cancer Center, Houston, TX) and cultured as described previously (22). Ascites were collected from women undergoing surgical procedures at Prentice Women's Hospital (Chicago, IL) for gynecologic indications with institutional review board–approved consent. Preoperative and intraoperative ascites were collected under sterile conditions and frozen at -20°C . Immunohistochemical analysis was done retrospectively on tumor tissue microarrays prepared by the Pathology Core Facility of the Robert H. Lurie Comprehensive Cancer Center at Northwestern University assembled from high-grade (2 or 3) tumor tissue originally taken for routine diagnostic purposes. Samples were prepared as described previously (22). Banked ascites and primary tumor tissues were not matched with respect to donor. Immunohistochemical staining with antibodies to MMP-9 (1:200 dilution; LabVision, Fremont, CA) or E-cadherin (1:200 dilution; clone NCH-38, DakoCytomation, Carpinteria, CA) was done according to standard procedures. Breast carcinoma and colon carcinoma were used as positive controls for MMP-9 and E-cadherin, respectively. Analysis of tissue sections was done by light microscopy by a pathologist (B.P.A.) without prior knowledge of the clinical variables. Scoring of MMP-9 or E-cadherin was assigned according to the intensity of the staining and graded 0, 1+ (weak), 2+ (moderate), or 3+ (strong).

Western blot analysis and E-cadherin ELISA. Western blot analysis was done as described previously (22). Western blots were quantified using ImageJ (U.S. NIH, Bethesda, MD). Ascites samples from 47 patients were analyzed for sE-cad using a human E-cadherin EIA kit (Invitrogen) according to the manufacturer's specifications.

Antibody purification and antibody adsorption to microbeads. TS2/16.2.1 hybridoma cells that produce β_1 integrin-specific antibody were obtained from American Type Culture Collection (Manassas, VA) and maintained in RPMI 1640 (Invitrogen), 10% heat-inactivated, low IgG fetal bovine serum (FBS; Invitrogen), sodium pyruvate, glutamine (Cellgro by Mediatech, Herndon, VA), and penicillin/streptomycin at 37°C in 5% CO₂. The resulting conditioned medium was loaded onto a HiTrap Protein G HP column (GE Healthcare, Piscataway, NJ) at 4°C using a Fast Protein Liquid Chromatography system. The column was washed with 100 mmol/L Tris (pH 8) and antibody was eluted with 150 mmol/L glycine (pH 3). Fractions were collected and buffered in 1 mol/L Tris (pH 8) and 1 mmol/L CaCl₂. Antibodies to α_2 , α_3 , or β_1 integrin and control IgG were passively adsorbed onto polybead amino 3.0 micron microspheres (2.59% solids latex; Polysciences, Inc., Warrington, PA) using the reagents in the glutaraldehyde kit for amino beads and blue-dyed beads (Polysciences, Inc.) and the protocol described previously (23).

Biotin surface labeling. To label cell surface proteins, cells were incubated with the non-cell-permeable biotin analogue Sulfo-NHS-LC-Biotin (1 mg/mL) for 25 min on ice, washed thrice in cold 100 mmol/L glycine in PBS and once in cold PBS, and lysed in modified radioimmunoprecipitation assay (mRIPA) buffer [50 mmol/L Tris (pH 7.5), 150 mmol/L NaCl, 1% Triton X-100, 5 mmol/L EDTA]. Equivalent amounts (50–70 μg) of lysate, as determined by the Bio-Rad (Hercules, CA) protein assay, were incubated with 25 to 30 μL NeutrAvidin protein overnight at 4° with gentle agitation. The NeutrAvidin biotin-labeled lysate complex was then washed five times in mRIPA lysis buffer, resuspended in mRIPA lysis buffer plus sample dilution buffer with 2-mercaptoethanol, and prepared for Western blot analysis.

E-cadherin ectodomain generation and immunoprecipitation. Cells were plated in six-well plates at 60% to 70% confluence, pretreated with inhibitors or vehicle overnight, and then treated with anti-integrin subunit-specific antibody-coated beads to induce integrin aggregation or with control IgG beads. At the indicated time point, the total volume of conditioned media (1 mL) was collected and centrifuged for 5 min. Similar conditions were used for treatment of cells with exogenous MMP-9, except that an inhibitor cocktail was added to block proteinase activity followed by incubation on ice for 20 min before centrifugation. Conditioned media (1 mL) were incubated with 2.5 μg anti-E-cadherin (HECD-1) for 3 h at room temperature and then with 20 μL Sepharose 4B FastFlow recombinant protein G for an additional hour at room temperature. The antibody-sepharose protein G complex was washed five times in PBS, resuspended in mRIPA lysis buffer plus sample dilution buffer with 2-mercaptoethanol, and prepared for Western blot analysis.

Gelatin zymography. Cells were plated at 60% to 70% confluence in 12-well plates and cultured in serum-free MEM overnight before the addition of integrin antibody-coated beads for an additional 36 to 40 h. Conditioned media were electrophoresed under nonreducing conditions on gelatin-containing polyacrylamide gels as described previously (22). Under serum-free conditions, MMP-9 is detected in the proenzyme form (24).

Purification of recombinant E-cadherin ectodomain-Fc chimeric protein (hEcad-Fc). Chinese hamster ovary cells stably expressing recombinant E-cadherin ectodomain-Fc chimeric protein (hEcad-Fc, previously designated HEEC1-5Fc) were generously provided by Dr. Barry Gumbiner (University of Virginia, Charlottesville, VA; ref. 25) and maintained in Ham's F12 medium (Invitrogen), 10% low IgG FBS, and penicillin/streptomycin at 37°C in 5% CO₂. For affinity purification of hEcad-Fc, the resulting conditioned medium was loaded onto a column containing rProtein A-Sepharose FastFlow (GE Healthcare) at 4°C , washed, eluted, and collected according to the manufacturer's specifications. Fractions containing hEcad-Fc protein, as determined by SDS-PAGE analysis, were pooled, desalted, and concentrated using Microcon YM-10 concentrators.

Immunofluorescence. Cells were plated at 60% to 70% confluence on 22-mm² glass coverslips placed in six-well tissue culture plates, cultured in serum-free MEM overnight, and then treated with 12 $\mu\text{g}/\text{mL}$ hEcad-Fc or mouse IgG for 24 to 48 h. Cells were gently washed in PBS, fixed in ice-cold methanol at -20°C for 5 min, washed in PBS, and blocked in PBS/1% BSA

for 1 h at room temperature followed by the addition of anti-E-cadherin (clone 4A2C7; 1:300 dilution in PBS/1% BSA) for 90 min at 37°C. After two washes in PBS, coverslips were incubated with Alexa Fluor 488 goat anti-mouse IgG (1:500 dilution in PBS/1% BSA) in the dark at room temperature for 30 min. Coverslips were washed in PBS twice and in distilled water once, fixed using Vectashield mounting medium for fluorescence with 4',6-diamidino-2-phenylindole (Vector Laboratories, Burlingame, CA), and visualized using a Zeiss (Thornwood, NY) Axiovert 200 microscope.

Results

E-cadherin expression and processing in the ovarian tumor microenvironment. Aberrant epithelial differentiation is an early

event in ovarian carcinogenesis; thus, in contrast to most carcinomas that lose E-cadherin expression with progression (7), E-cadherin is abundant in primary ovarian carcinomas (Fig. 1A; refs. 8–10, 26). Samples of primary ovarian tumors from 137 patients (70 serous carcinoma, 42 endometrioid carcinoma, 16 clear cell carcinoma, and 9 mucinous carcinoma) were examined for E-cadherin immunoreactivity. The vast majority of ovarian tumors (86%) displayed positive E-cadherin immunoreactivity, and E-cadherin expression was high (3+ or 2+) in 72% of patients overall (70% of serous, 62% of endometrioid, 94% of clear cell, and 100% of mucinous). A representative example of each histotype stained for E-cadherin and a serial H&E section are shown in Fig. 1A.

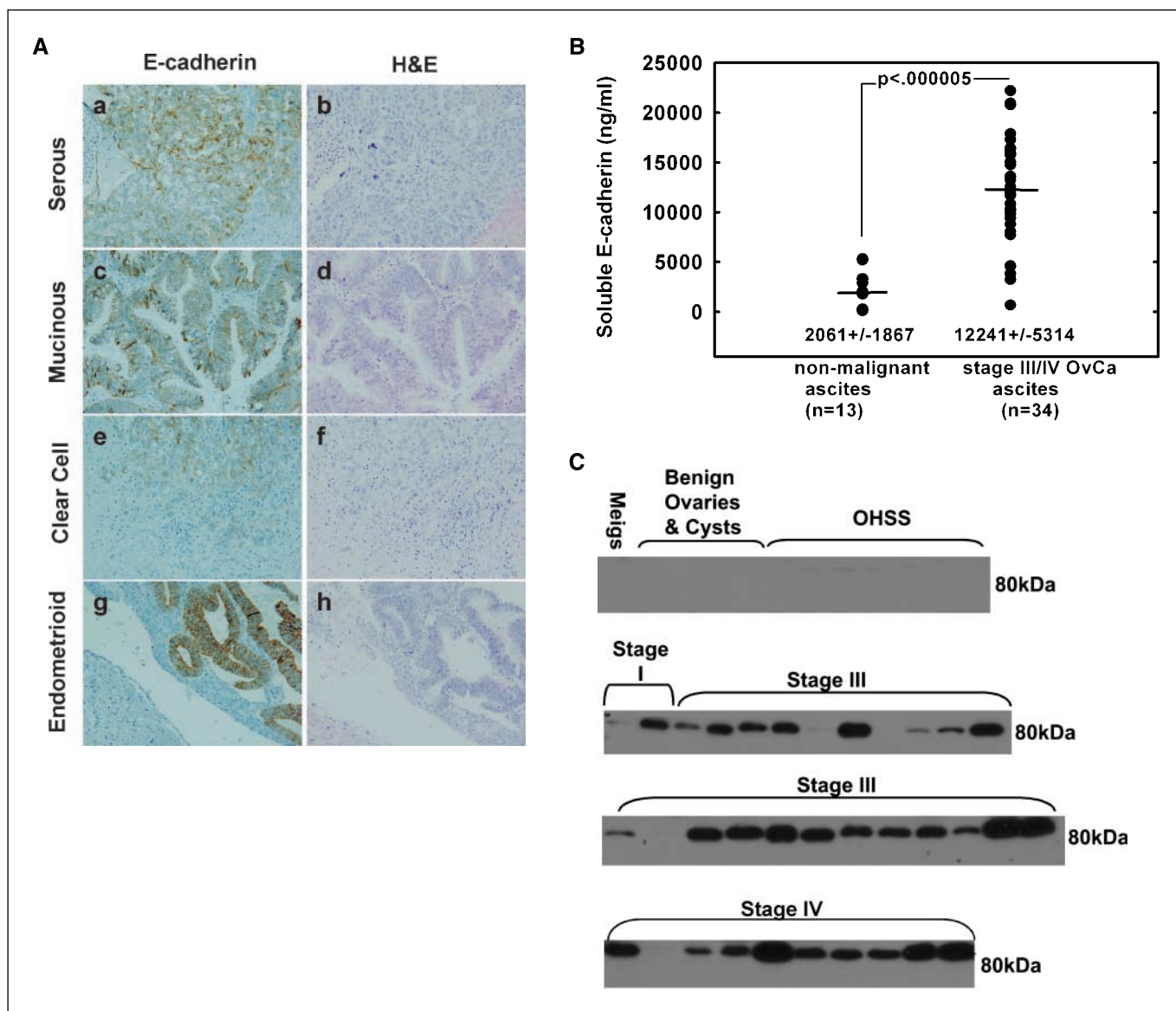


Figure 1. E-cadherin expression in ascites and tumor samples from ovarian cancer patients. *A*, samples were stained with antibodies to E-cadherin (1:200; *a*, *c*, *e*, and *g*) or H&E (*b*, *d*, *f*, and *h*) as described in Materials and Methods. *a* and *b*, serous carcinoma; *c* and *d*, mucinous carcinoma; *e* and *f*, clear cell carcinoma; *g* and *h*, endometrioid carcinoma. *B* and *C*, nonmalignant ascites samples ($n = 13$) were obtained from women diagnosed with benign ovarian cysts, OHSS, or Meigs syndrome (*Meigs*). Malignant ascites samples ($n = 34$) were obtained from women diagnosed with ovarian cancer at either stage I, III, or IV. *B*, patient ascites samples were analyzed using ELISA according to the manufacturer's specifications to determine the levels of sE-cad. *C*, ascites samples ($1 \mu\text{L}$) were diluted in PBS, electrophoresed on 9% SDS-PAGE gels, transferred to polyvinylidene difluoride (PVDF) membranes, and immunoblotted with anti-E-cadherin (HECD-1; 1:4,000) followed by peroxidase-conjugated secondary antibody (1:5,000) and enhanced chemiluminescence (ECL) detection. Whole-cell lysates from the OVCA433 cell lines served as a positive control for full-length (120 kDa) E-cadherin (data not shown).

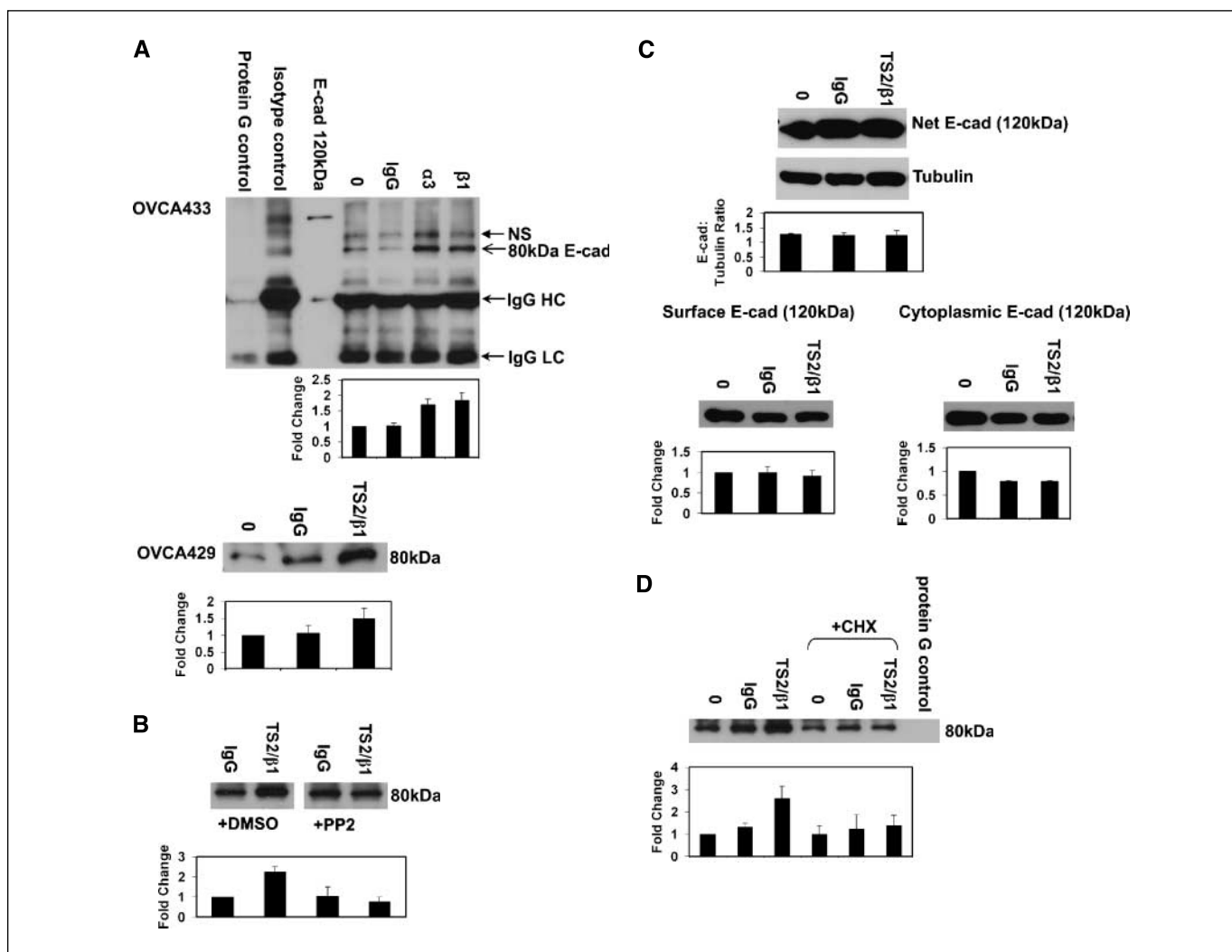


Figure 2. Engagement of collagen-binding integrins promotes E-cadherin ectodomain shedding. *A*, *top*, OVCA433 cells were treated with control IgG, anti-integrin α_3 , or anti-integrin β_1 immobilized to latex beads for 20 h. The 80-kDa E-cadherin ectodomain was immunoprecipitated from the conditioned media as described in Materials and Methods. Controls include conditioned media incubated with protein G-Sepharose beads alone to verify specificity of the E-cadherin antibody (*lane 1*) and conditioned media subjected to immunoprecipitation with mouse IgG to show isotype specificity (*lane 2*). Immunoprecipitates were electrophoresed on a 9% SDS-PAGE gel, transferred to a PVDF membrane, and immunoblotted with anti-E-cadherin (HECD-1; 1:4,000) followed by peroxidase-conjugated secondary antibody (1:5,000) and ECL detection. OVCA433 whole-cell lysates were used as a positive control for full-length E-cadherin (*lane 3*) and the IgG heavy and light chains are shown as loading controls (*lanes 4–7*). Representative Western blot and densitometric quantification of the 80-kDa ectodomain. Results were normalized against the densitometric reading for untreated cells (*lane 4*) and represent four independent experiments. *NS*, nonspecific band; *IgG HC*, IgG heavy chain; *IgG LC*, IgG light chain. *Bottom*, OVCA429 cells were treated with control IgG or anti-integrin β_1 /TS2 immobilized to latex beads for 20 h. The 80-kDa E-cadherin ectodomain was immunoprecipitated from the conditioned media as described in Materials and Methods. Immunoprecipitates were electrophoresed on a 9% SDS-PAGE gel, transferred to a PVDF membrane, and immunoblotted with anti-E-cadherin (HECD-1; 1:4,000) followed by peroxidase-conjugated secondary antibody (1:5,000) and ECL detection. Representative Western blot and densitometric quantification of the 80-kDa ectodomain. Results were normalized against the densitometric reading for untreated cells (*lane 1*) and represent three independent experiments. *B*, OVCA433 cells were preincubated with PP2 (10 μ mol/L) or DMSO before treatment with either control IgG or TS2/ β_1 antibody immobilized on latex beads for 20 h. The 80-kDa E-cadherin ectodomain was immunoprecipitated from the conditioned media as described in Materials and Methods. Immunoprecipitates were electrophoresed on a 9% SDS-PAGE gel, transferred to a PVDF membrane, and immunoblotted with anti-E-cadherin (HECD-1; 1:4,000) followed by peroxidase-conjugated secondary antibody (1:5,000) and ECL detection. Representative Western blot and densitometric quantification of the 80-kDa ectodomain. Results were normalized against the densitometric reading for cells treated with control IgG beads (*lane 1*) and represent three independent experiments. *C*, OVCA433 cells were treated with either control IgG or TS2/ β_1 antibody immobilized on latex beads for 20 h. *Top*, whole-cell lysates (20 μ g) were electrophoresed on a 9% SDS-PAGE gel, transferred to a PVDF membrane, and immunoblotted with anti-E-cadherin (HECD-1; 1:4,000) followed by peroxidase-conjugated secondary antibody (1:5,000) and ECL detection. Full-length E-cadherin (120 kDa) was detected. Tubulin was used as a loading control. Representative Western blot and densitometric quantification of full-length E-cadherin. Results were normalized against the densitometric reading for untreated cells (*lane 1*) and represent three independent experiments. To evaluate the amount of E-cadherin present on the cell surface, cells were surface biotinylated and lysed, and lysates (50 μ g) were incubated with Neutravidin. Following incubation, the Neutravidin conjugated lysates and resulting supernatants were electrophoresed on a 9% SDS-PAGE gel, transferred to a PVDF membrane, and immunoblotted with anti-E-cadherin (HECD-1; 1:4,000) followed by peroxidase-conjugated secondary antibody (1:5,000) and ECL detection to examine the surface E-cadherin expression (*bottom*) and cytoplasmic E-cadherin expression (*bottom*), respectively. Full-length E-cadherin (120 kDa) was detected in both populations. Representative Western blot and densitometric quantification of full-length E-cadherin. Results were normalized against the densitometric reading for untreated cells (*lane 1*). Surface and cytoplasmic E-cadherin results represent three and two independent experiments, respectively. *D*, OVCA433 cells were preincubated with cycloheximide (CHX; 20 μ mol/L) or DMSO before treatment with either control IgG or TS2/ β_1 antibody immobilized on latex beads for 20 h. The 80-kDa E-cadherin ectodomain was immunoprecipitated from the conditioned medium as described in Materials and Methods. Immunoprecipitates were electrophoresed on a 9% SDS-PAGE gel, transferred to a PVDF membrane, and immunoblotted with anti-E-cadherin (HECD-1; 1:4,000) followed by peroxidase-conjugated secondary antibody (1:5,000) and ECL detection. Conditioned medium was also incubated with Protein G-Sepharose only (protein G control) to show the specificity of the E-cadherin immunoprecipitation. Representative Western blot and densitometric quantification of the 80-kDa Ectodomain. Results were normalized against the densitometric reading for untreated cells (*lane 1*) and represent four independent experiments.

E-cadherin expression was maintained in the majority of tumor samples regardless of tumor histotype or Federation Internationale des Gynaecologues et Obstetristes stage, consistent with the observation that genetic mutations in the *E-cadherin* gene that result in loss of expression are rare in ovarian tumors (11).

Single cells and multicellular aggregates are shed from primary ovarian tumors and adhere via integrins to submesothelial collagens, suggesting that post-translational modulation of E-cadherin may occur to alter adhesive function and thereby promote *i.p.* dissemination. Indeed, a sE-cad ectodomain fragment (sE-cad) of unreported size has been detected in the serum of patients with gastric cancer, multiple myeloma, and melanoma (27–29). Cystic fluid from patients with benign or malignant cystic ovarian masses also contained elevated sE-cad (12, 13), although no significant differences were observed in sera (12, 13). ELISA and immunoblot analysis were used to detect sE-cad in a total of 47 ascites samples from women with benign ovarian cysts, Meig's syndrome, ovarian hyperstimulation syndrome (OHSS), or stage I, III, and IV ovarian cancer. sE-cad levels were significantly elevated (6-fold; $P < 0.005$) in ascites from women with ovarian cancer compared with ascites from women with OHSS or benign ovarian cysts (Fig. 1B). Immunoblot analysis was then used to evaluate the integrity of the sE-cad fragment(s) detected by ELISA using an antibody to the E-cadherin extracellular region (HECD-1). A major 80-kDa E-cadherin ectodomain species was detected in the majority of ovarian cancer ascites samples but was not present in nonmalignant ascites (Fig. 1C). Full-length E-cadherin (containing the cytoplasmic domain) and degraded E-cadherin ectodomain fragments <80 kDa were not detected (data not shown).

Integrin clustering increases E-cadherin ectodomain shedding. The 80-kDa E-cadherin ectodomain is shed following proteolytic cleavage in several different cell types *in vitro* (17–21); however, the cellular events that regulate this process are not well characterized. As a consequence of *i.p.* metastasis, clustering of collagen-binding integrins $\alpha_2\beta_1$ and $\alpha_3\beta_1$ occurs when aggregates of cells attach to the collagen-rich submesothelial ECM (3). Integrins signal cellular responses by regulating the formation of signal transduction complexes on a cytoskeletal framework, and this integration of signaling and cytoskeletal events is dictated by the physical nature of the integrin-ligand interaction (14). Thus, integrin aggregation by an intact three-dimensional matrix can be modeled using integrin subunit-specific antibodies immobilized on beads (14). To evaluate the effect of integrin clustering on E-cadherin status, cells were treated with bead-immobilized subunit-specific antibodies to α_3 or β_1 integrin or control IgG. E-cadherin ectodomain shedding was then evaluated by immunoprecipitation of conditioned media using E-cadherin ectodomain-specific antibodies followed by Western blotting. Increased shedding of the E-cadherin ectodomain was observed following aggregation of collagen-binding integrins in two ovarian cancer cell lines (Fig. 2A). Previous studies have shown that Src activity is necessary for the disruption of cadherin-mediated cell adhesion in cancer cells (30, 31), and integrin signaling has been linked to Src-induced junction disruption (31). Integrin aggregation in the presence of the Src family kinase inhibitor PP2 decreased E-cadherin ectodomain shedding (Fig. 2B), suggesting that Src kinase activity is also needed to promote E-cadherin ectodomain shedding.

To investigate whether E-cadherin ectodomain shedding resulted in a net loss of cellular E-cadherin protein, whole-cell lysates were

evaluated following integrin aggregation. No net change in total full-length (120 kDa) E-cadherin expression was observed in whole-cell lysates following integrin aggregation (Fig. 2C, top). This was confirmed by surface biotinylation to distinguish cell surface and cytoplasmic pools of E-cadherin. Despite increased ectodomain shedding observed at 20 h, surface and cytoplasmic expression of full-length E-cadherin was not modulated at this time point (Fig. 2C, bottom). Long-term culture (1 month) of OVCA433 cells on thin layer collagen also did not induce a permanent reduction in net or surface E-cadherin expression.⁶ As these results suggested that new protein synthesis replenishes the shed E-cadherin, to test this hypothesis aggregation of β_1 integrins was induced in the presence of the protein synthesis inhibitor cycloheximide, and the resulting conditioned media were analyzed for the E-cadherin ectodomain. Integrin-induced E-cadherin ectodomain shedding was reduced by cycloheximide treatment (Fig. 2D). Together, these results support the hypothesis that integrins act as upstream modulators of E-cadherin ectodomain shedding that is dependent on new protein synthesis.

MMP-9-dependent generation of E-cadherin ectodomain following integrin aggregation. Metalloproteinase-dependent E-cadherin ectodomain shedding has been observed in various cell types; however, the cellular events that regulate this process are not well characterized (17–21). We have shown previously that multivalent aggregation of collagen-binding integrins regulates MMP expression by ovarian cancer cells (15, 16). Aggregation of collagen-binding integrins in the presence of the broad spectrum MMP inhibitor GM6001 reduced E-cadherin ectodomain shedding, implicating integrin-regulated MMP activity in this process (Fig. 3A). Integrin clustering increased expression of MMP-9 (Fig. 3B and C) without altering MMP-2 and MMP-14 (data not shown) and MMP-9 immunoreactivity was prevalent in the majority of human ovarian tumors analyzed (Fig. 3D). Although MMP-9 is commonly expressed by stromal elements in many tumors (32), *in situ* hybridization analyses have provided definitive evidence for robust expression of MMP-9 by malignant ovarian epithelium (33–35). This is supported by immunohistochemical analysis of 141 primary ovarian tumors (71 serous tumors, 43 endometrioid tumors, 18 clear cell tumors, and 9 mucinous tumors), which shows MMP-9 expression in 74% of specimens (representative examples are shown in Fig. 3D). MMP-9 expression was high (2+ or 3+) in 28% of serous tumors, 21% of endometrioid tumors, 11% clear cell tumors, and 22% of mucinous tumors. Furthermore, total MMP-9 expression was elevated ~2-fold in the ascites of ovarian cancer patients when compared with the ascites from women with benign ovarian cysts.⁶ These findings suggest that MMP-9 may be an important factor in the ovarian tumor microenvironment that contributes to E-cadherin ectodomain shedding.

To evaluate the potential contribution of MMP-9 to E-cadherin cleavage, integrin aggregation was induced in the presence of a MMP-9 function blocking antibody. Specific blocking of MMP-9 activity abolished the integrin-mediated increase in shed E-cadherin ectodomain with little effect on basal ectodomain shedding (Fig. 4A). Because the MMP-9 blocking antibody inhibits extracellular MMP-9 activity, these data show MMP-9-dependent cleavage of surface-associated, rather than intracellular, E-cadherin.

⁶ Unpublished results.

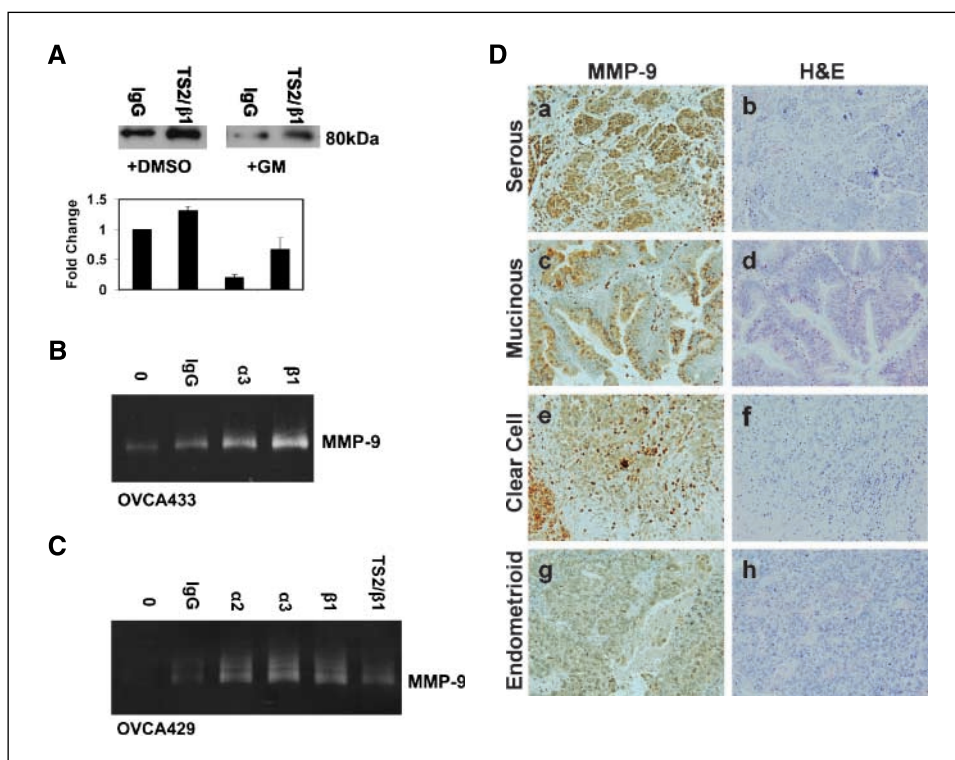


Figure 3. MMP-9 expression in ovarian cancer cell lines and tumor samples. *A*, OVCA433 cells were preincubated with GM6001 (50 μ mol/L) or DMSO before treatment with either control IgG or TS2/ β ₁ antibody immobilized on latex beads for 20 h. The 80-kDa E-cadherin ectodomain was immunoprecipitated from the conditioned media as described in Materials and Methods. Immunoprecipitates were electrophoresed on a 9% SDS-PAGE gel, transferred to a PVDF membrane, and immunoblotted with anti-E-cadherin (HECD-1; 1:4,000) followed by peroxidase-conjugated secondary antibody (1:5,000) and ECL detection. Representative Western blot and densitometric quantification of the 80-kDa Ectodomain. Results were normalized against the densitometric reading for cells treated with control IgG beads (*lane 1*) and represent three independent experiments. *B*, OVCA433 cells were treated with control IgG, anti-integrin α ₃, or anti-integrin β ₁ immobilized to latex beads for 40 h. *C*, OVCA429 cells were treated with control IgG, anti-integrin α ₂, anti-integrin α ₃, anti-integrin β ₁, or anti-integrin β ₁/TS2 immobilized to latex beads for 36 h. *B* and *C*, the resulting conditioned media (30 μ L) were analyzed for MMP-9 expression using gelatin zymography. Under serum-free conditions, the proenzyme form of MMP-9 is detected. *D*, tumor samples were stained with antibodies to MMP-9 (1:200; *a*, *c*, *e*, and *g*) or H&E (*b*, *d*, *f*, and *h*) as described in Materials and Methods. *a* and *b*, serous carcinoma; *c* and *d*, mucinous carcinoma; *e* and *f*, clear cell carcinoma; *g* and *h*, endometrioid carcinoma.

To further verify MMP-9-catalyzed E-cadherin ectodomain shedding, cells were incubated with exogenous MMP-9 at 100 ng/mL, which was found to be the average concentration of MMP-9 in ovarian cancer ascites.⁶ A substantial increase in the shed E-cadherin ectodomain was catalyzed by MMP-9 and the generation of the ectodomain was inhibited by the MMP inhibitor GM6001 (Fig. 4*B*). These data support a role for both endogenous and exogenous MMP-9 in promoting E-cadherin ectodomain shedding. Additional comparison of tumors with high levels of MMP-9 immunoreactivity (scored 2+ or 3+ in the analysis above; $n = 68$) and serial sections stained with anti-E-cadherin antibodies support these *in vitro* data. Although overall a statistically significant negative correlation between MMP-9 and E-cadherin staining was not shown, evaluation of serial sections showed that 51% of tumors with high MMP-9 expression exhibit low or absent E-cadherin staining (0 or 1+) and all MMP-9-positive tumors exhibited focal areas of high MMP-9 positivity colocalized with low E-cadherin staining (Fig. 4*C*). Together, these findings support the hypothesis that MMP-9 is a regulator of E-cadherin ectodomain shedding in the ovarian tumor microenvironment.

The shed ectodomain disrupts preformed adherens junctions.

In contrast to other tumors wherein shed E-cadherin ectodomain is released into the circulation, primary ovarian tumors maintain direct contact with sE-cad-rich ascites at high concentration

(average 12 μ g/mL; Fig. 1*B*). This unique microenvironment provides a physiologically relevant model system to assess the potential functional contribution of the E-cadherin ectodomain to ovarian cancer pathobiology. To test the hypothesis that the ectodomain may interact with endogenous cellular E-cadherin, cells were treated with a recombinant form of the human E-cadherin 80-kDa ectodomain (designated hEcad-Fc), and changes in junctional integrity were evaluated using immunofluorescence microscopy. Preformed junctions were disrupted by hEcad-Fc (Fig. 5*A*, *b* and *d*; *B*, *f* and *h*) at concentrations representing the average value detected in ovarian cancer patient ascites (12 μ g/mL; Fig. 1*B*). Morphologic changes were also apparent at 48 h, with evidence of increased cell dispersion relative to more compact colonies maintained by control cells (Fig. 5*A*, *d*). These data suggest that, although integrin-mediated E-cadherin ectodomain shedding does not result in a net loss of cellular E-cadherin (Fig. 2*C* and *D*), the ectodomain remaining in the ovarian tumor microenvironment promotes cell-cell junction disruption, thereby potentially enhancing *i.p.* dissemination.

Discussion

The majority of women with ovarian cancer present at diagnosis with established metastases throughout the peritoneal cavity (1), suggesting that a more detailed understanding of factors

that promote i.p. dissemination may result in therapeutic strategies that target metastasis. Reversible modulation of cell-matrix adhesion, cell-cell adhesion, and proteolytic activity are key events in ovarian cancer metastasis. Shedding of single cells and multicellular aggregates from the primary tumor requires junction disruption, whereas i.p. adhesion and localized invasion are necessary to establish metastases (3). Following disruption of the mesothelial monolayer, disseminated ovarian tumor cells preferentially adhere to the exposed submesothelial ECM via collagen-binding integrins $\alpha_2\beta_1$ and $\alpha_3\beta_1$ and subsequently anchor at these new sites to establish metastases throughout the peritoneal cavity (3). As ovarian cancer induces a fibroproliferative response characterized by enhanced synthesis of interstitial collagens in the peritoneal cavity, EOC cells or multicellular aggregates in ascites also encounter collagen species that engage cellular integrins (36). Our previous data showing integrin-regulated proteinase expression in EOC cells (15, 16) suggested a potential functional link between integrin engagement, enhanced proteolytic activity, and modulation of E-cadherin function. Although several proteinases have been reported to cleave E-cadherin (17–21), upstream regulators of the proteinase(s) that promote ectodomain shedding are largely unexplored. The current

data support the hypothesis that integrin-regulated MMP-9-catalyzed E-cadherin ectodomain shedding may potentiate metastatic dissemination of EOC.

Although the current data show a role for MMP-9 expressed by EOC cells in E-cadherin ectodomain shedding, multiple cell types may contribute to MMP-9 expression in the ovarian tumor microenvironment. MMP-9 is produced by epithelial cells, fibroblasts, endothelial cells, and peritoneal mesothelial cells (37, 38). Similar to murine model studies of squamous cell carcinogenesis showing that inflammatory cells in the stroma are the primary MMP-9 source (39), stromal MMP-9 from tumor-infiltrating macrophages was also shown to promote angiogenesis and proliferation of ovarian tumors in a murine xenograft model (40), although extensive macrophage infiltration was not apparent in the human tumors evaluated in the current study (Fig. 3D). In human ovarian tumors, MMP-9 immunoreactivity has been observed in both the epithelial and the stromal compartments (41, 42) and MMP-9 activity has been detected by gelatin zymography (35, 43). Epithelial MMP-9 immunoreactivity was increased in malignant ovarian tumors relative to borderline ovarian tumors (41). Three distinct studies have also shown MMP-9 mRNA expression in the epithelial compartment of human EOC tumors

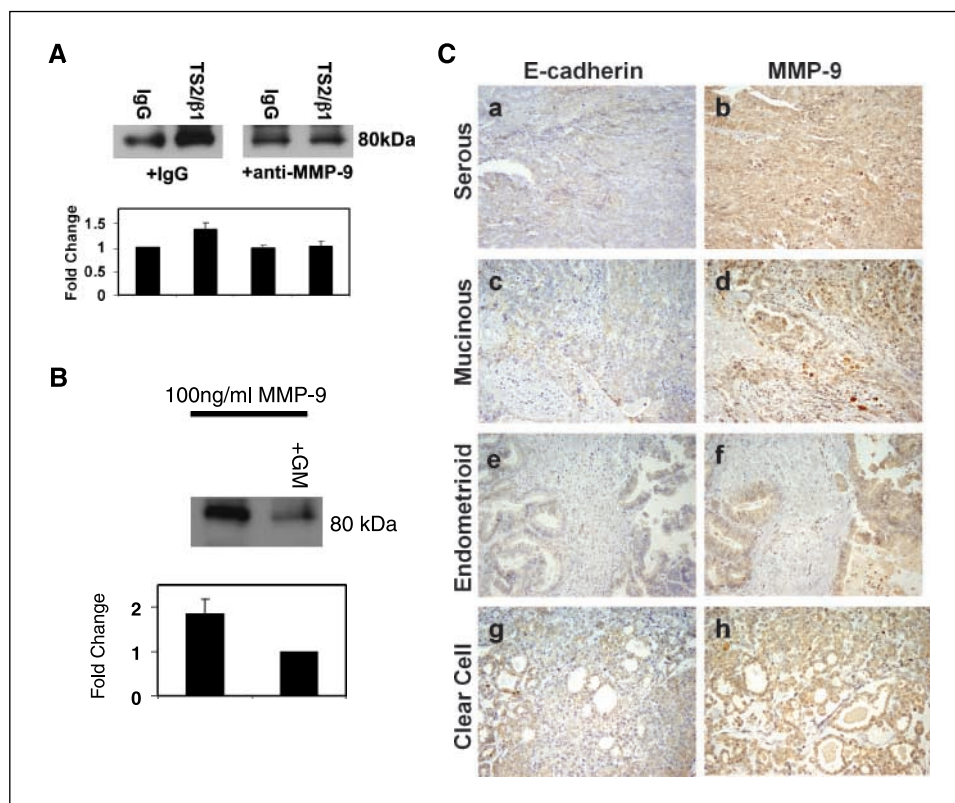


Figure 4. MMP-9 promotes integrin-mediated E-cadherin ectodomain shedding. **A**, OVCA433 cells were preincubated with anti-MMP-9 (10 μ g/mL) or control IgG before treatment with either control IgG or TS2 β 1 antibody immobilized on latex beads for 20 h. The 80-kDa E-cadherin ectodomain was immunoprecipitated from the conditioned media as described in Materials and Methods. Immunoprecipitates were electrophoresed on a 9% SDS-PAGE gel, transferred to a PVDF membrane, and immunoblotted with anti-E-cadherin (HECD-1; 1:4,000) followed by peroxidase-conjugated secondary antibody (1:5,000) and ECL detection. Representative Western blot and densitometric quantification of the 80-kDa ectodomain. Results were normalized against the densitometric reading for cells treated with control IgG beads (*lane 1*) and represent three independent experiments. **B**, OVCA433 cells were preincubated with GM6001 (50 μ mol/L) or DMSO before treatment with recombinant activated MMP-9 (100 ng/mL) for 24 h. The 80-kDa E-cadherin ectodomain was immunoprecipitated from the conditioned media as described in Materials and Methods. Immunoprecipitates were electrophoresed on a 9% SDS-PAGE gel, transferred to a PVDF membrane, and immunoblotted with anti-E-cadherin (HECD-1; 1:4,000) followed by peroxidase-conjugated secondary antibody (1:5,000) and ECL detection. Representative Western blot and densitometric quantification of the 80-kDa ectodomain. Results were normalized against the densitometric reading for cells treated with MMP-9 and GM6001 (*GM*; *lane 2*) and represent two independent experiments. **C**, serial sections of ovarian tumor samples were stained with antibodies to E-cadherin (1:200; *a*, *c*, *e*, and *g*) or MMP-9 (1:200; *b*, *d*, *f*, and *h*) as described in Materials and Methods. *a* and *b*, serous carcinoma; *c* and *d*, mucinous carcinoma; *e* and *f*, endometrioid carcinoma; *g* and *h*, clear cell carcinoma.

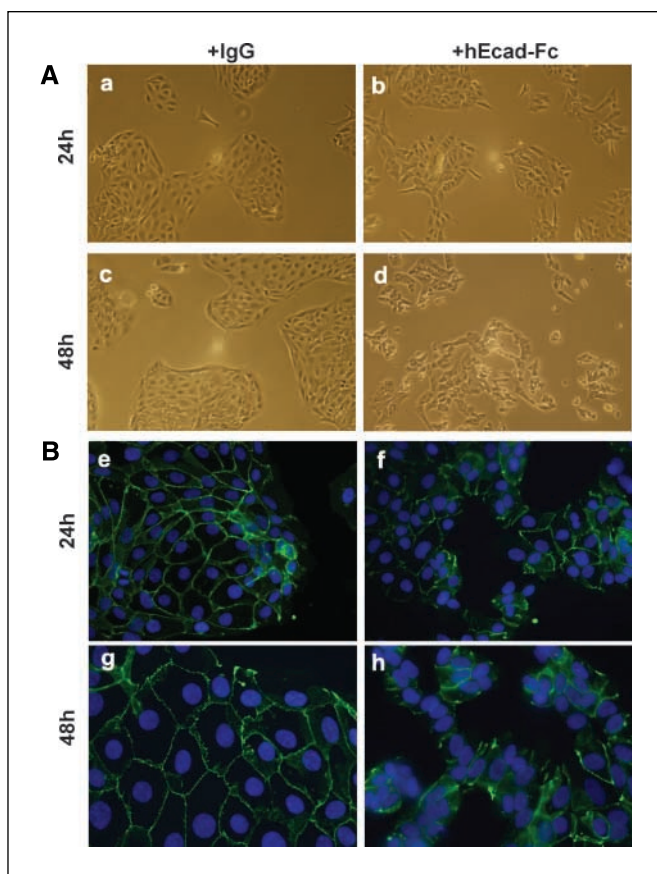


Figure 5. The shed E-cadherin ectodomain promotes cell junction disruption and cell dissemination. OVCA433 cells were plated on glass coverslips at ~60% confluence. The next day, cells were incubated in serum-free media overnight before treatment with hEcad-Fc (12 μ g/mL) or control IgG for 24 and 48 h. **A**, phase-contrast images of cells were taken at 24 h (*a* and *b*) and 48 h (*c* and *d*). Magnification, $\times 10$. **B**, cells were then processed for immunofluorescence using anti-cytoplasmic E-cadherin (1:300 dilution) and FITC-conjugated IgG, as described in Materials and Methods, at 24 h (*e* and *f*) and 48 h (*g* and *h*). Magnification, $\times 40$.

by *in situ* hybridization analysis (33–35). These data are supported by studies using short-term primary cultures of EOC cells obtained from primary tumors, ascites, and peritoneal metastases, showing MMP-9 expression in early passage tumor epithelial cells decreased with increasing passage in culture, indicative of regulation by a component(s) of the *in vivo* tumor microenvironment (44). Regardless of the cellular source of the secreted proteinase, high MMP-9 levels in ovarian tumor tissues and ascites are associated with disease recurrence and poor patient survival (45). Further, our data show that both EOC-expressed and exogenous MMP-9 effectively catalyze E-cadherin ectodomain shedding.

c-Src and Src family kinases participate in integrin-mediated transmission of signals from the extracellular microenvironment, either via focal adhesion kinase (FAK) activation (46) or by a FAK-independent direct interaction between Src and the β integrin cytoplasmic tail that induces Src activation and stabilizes the activated kinase following integrin clustering (47). Activated Src has been shown to disrupt cadherin-catenin complexes in human colon cancer cells (30) and recent studies show Src-mediated disruption of cell-cell junctions in colon cancer cells that is dependent on integrin signaling (31). As the current data show

that inhibition of Src activity blocked integrin-induced E-cadherin ectodomain shedding, it is interesting to speculate that Src activity functions to initiate junction dissolution, thereby facilitating access of MMP-9 to the E-cadherin cleavage site at the cell surface.

Integrin-induced E-cadherin ectodomain shedding does not result in a net loss of E-cadherin, as new protein synthesis occurs to replace the shed adhesion molecule. However, other factors prevalent in ascites, including lysophosphatidic acid and epidermal growth factor, enhance MMP-9 expression by ovarian cancer cells (48)⁶ and may thereby contribute to E-cadherin ectodomain shedding, resulting in further modulation of E-cadherin function. Although an overall negative correlation between MMP-9 and E-cadherin immunoreactivity was not observed, evaluation of serial sections showed staining heterogeneity such that all MMP-9-positive tumors exhibited focal areas of high MMP-9 positivity colocalized with low or absent E-cadherin staining, supporting the hypothesis that MMP-9 is a regulator of E-cadherin ectodomain shedding in the ovarian tumor microenvironment.

It has been proposed that the gain of E-cadherin expression observed during ovarian tumorigenesis is advantageous for metastatic progression by enabling survival of multicellular aggregates in suspension (ascites), inducing attachment to other cells in the peritoneal cavity, and promoting cohort migration that facilitates metastatic implantation (2). Results from a recent study reported that human ovarian carcinomas without metastasis exhibit E-cadherin membrane expression, whereas E-cadherin staining is either cytoplasmic or absent in metastatic ovarian carcinomas (26), suggesting that sustained E-cadherin expression and/or function is not necessary following tumor cell attachment and anchoring at new sites. Although immunofluorescence images were not provided, it is interesting to note that this study used the HECD-1 antibody, which detects the E-cadherin extracellular domain, and the results are thereby indicative of either a defect in membrane trafficking or, alternatively, enhanced E-cadherin internalization in metastatic lesions that retain E-cadherin positivity. E-cadherin-negative samples in the Marques et al. (26) study could result from epigenetic silencing of E-cadherin expression (49, 50) and/or may represent lesions with levels of E-cadherin ectodomain shedding that exceed rates of replenishment. Together with our current data showing high levels of shed E-cadherin ectodomain in ascites from women with ovarian cancer, these combined results indicate multiple complex mechanisms of E-cadherin regulation in ovarian tumors.

The shed E-cadherin ectodomain, at concentrations found in human carcinomatous ascites, induces characteristics of a phenotypic epithelial-mesenchymal transition (EMT) in ovarian cancer cells, such as junction disruption and morphologic alteration to a migratory phenotype. Similarly, in both murine mammary epithelium and a rat cataract model, E-cadherin ectodomain shedding was found to promote an EMT (18, 51). Although the association between EMT and E-cadherin ectodomain shedding has not been extensively evaluated in human cancer models, sE-cad is elevated in the bodily fluids of cancer patients and is associated with poor prognosis or the development of metastasis (12, 13, 27–29). *In vitro*, the E-cadherin ectodomain has been linked with increased migration, invasion, proliferation, MMP activity, and disrupted adhesion in various cell lines (19, 52–55). sE-cad levels are elevated in the cystic fluid from borderline and

malignant ovarian tumors when compared with benign cysts and cystadenomas (12), suggesting that this distinction may have diagnostic value preoperatively.

The current data provide additional evidence for high levels of sE-cad in the ovarian tumor microenvironment and show that, in contrast to other tumors wherein shed E-cadherin ectodomain is released into the circulation, primary ovarian tumors maintain direct contact with sE-cad-rich ascites at high concentration. Our data support a model for increased E-cadherin ectodomain shedding as tumor cells disseminate from the primary tumor, adhere to the exposed collagen-rich submesothelial matrix, and up-regulate MMP-9 activity as a consequence of integrin clustering. As the primary tumor and both suspended and anchored metastatic cells maintain contact with sE-cad-rich ascites, high levels of sE-cad in the ovarian tumor microenviron-

ment may encourage further disaggregation of cells from the primary tumor or ascitic cancer cell spheroids, thereby enhancing metastatic dissemination.

Acknowledgments

Received 7/31/2006; revised 11/6/2006; accepted 12/15/2006.

Grant support: NIH/National Cancer Institute training grant T32CA09560 (J. Symowicz); NIH grants R01CA86984 and CA109545 (M.S. Stack) and CA90492 (L.G. Hudson); Phi Beta Psi research grant (M.S. Stack); and Gramm Travel Award from the Robert H. Lurie Comprehensive Cancer Center of Northwestern University (J. Symowicz).

The costs of publication of this article were defrayed in part by the payment of page charges. This article must therefore be hereby marked *advertisement* in accordance with 18 U.S.C. Section 1734 solely to indicate this fact.

We thank Dr. Cara Gottardi and Dr. Anjen Chenn (Northwestern University) for helpful discussions and Dr. Alfred Rademaker, director of the Biostatistics Core Facility of the Robert H. Lurie Comprehensive Cancer Center (Northwestern University), for statistical analyses.

References

- Fishman D, Borzorgi K. The scientific basis of early detection of epithelial ovarian cancer: the national ovarian cancer early detection program (NOCEDP). In: Stack MS, Fishman DA, editors. *Cancer treatment and research: ovarian cancer*. Boston: Kluwer Academic Publishers; 2002. p. 3–28.
- Naora H, Montell DJ. Ovarian cancer metastasis: integrating insights from disparate model organisms. *Nat Rev Cancer* 2005;5:355–66.
- Ghosh S, Wu Y, Stack MS. Ovarian Cancer-associated proteinases. In: Stack MS, Fishman DA, editors. *Cancer treatment and research: ovarian cancer*. Boston: Kluwer Academic Publishers; 2002. p. 331–54.
- Offner FA, Obrist P, Stadlmann S, et al. IL-6 secretion by human peritoneal mesothelial and ovarian cancer cells. *Cytokine* 1995;7:542–7.
- Mutsaers SE. Mesothelial cells: their structure, function, and role in serosal repair. *Respirology* 2002;7:171–91.
- Freedman RS, Deavers M, Liu J, Wang E. Peritoneal inflammation: a microenvironment for epithelial ovarian cancer (EOC). *J Transl Med* 2004;2:23.
- Auersperg N, Pan J, Grove BD, et al. E-cadherin induces mesenchymal-to-epithelial transition in human ovarian surface epithelium. *Proc Natl Acad Sci U S A* 1999;96:6249–54.
- Wong AST, Maines-Bandiera SL, Rosen B, et al. Constitutive and conditional cadherin expression in cultured human ovarian surface epithelium: influence of family history of ovarian cancer. *Int J Cancer* 1999;81:180–8.
- Maines-Bandiera SL, Auersperg N. Increased E-cadherin expression in ovarian surface epithelium: an early step in metaplasia and dysplasia? *Int J Gynecol Pathol* 1997;16:250–5.
- Imai T, Horiuchi A, Shiozawa T, et al. Elevated expression of E-cadherin and α -, β -, and γ -catenins in metastatic lesions compared with primary epithelial ovarian carcinomas. *Hum Pathol* 2004;35:1469–76.
- Wong AST, Auersperg N. Normal ovarian surface epithelium. In: Stack MS, Fishman DA, editors. *Cancer treatment and research: ovarian cancer*. Boston: Kluwer Academic Publishers; 2002. p. 161–84.
- Sundfeldt K, Ivarsson K, Rask K, et al. Higher levels of soluble E-cadherin in cyst fluid from malignant ovarian tumours than in benign cysts. *Anticancer Res* 2001;21:65–70.
- Darai E, Bringuier AF, Walker-Combrouze F, Feldmann G, Madelenat P, Scoazec, JY. Soluble adhesion molecules in serum and cyst fluid from patients with cystic tumours of the ovary. *Hum Reprod* 1998;13:2831–5.
- Yamada KM, Miyamoto S. Integrin transmembrane signaling and cytoskeletal control. *Curr Opin Cell Biol* 1995;7:681–9.
- Ellerbroek SM, Fishman DA, Kearns AS, Bafetti LM, Stack MS. Ovarian carcinoma regulation of matrix metalloproteinase-2 and membrane type 1 matrix metalloproteinase through β_1 integrin. *Cancer Res* 1999;59:1635–41.
- Ellerbroek SM, Wu YI, Overall CM, Stack MS. Functional interplay between type I collagen and cell surface matrix metalloproteinase activity. *J Biol Chem* 2001;276:24833–42.
- Damsky C, Richa J, Solter D, Knudsen K, Buck C. Identification and purification of a cell surface glycoprotein mediating intercellular adhesion in embryonic and adult tissue. *Cell* 1983;34:455–66.
- Lochter A, Galosy S, Muschler J, Freedman N, Werb Z, Bissell MJ. Matrix metalloproteinase stromelysin-1 triggers a cascade of molecular alterations that leads to stable epithelial-to-mesenchymal conversion and a premalignant phenotype in mammary epithelial cells. *J Cell Biol* 1997;139:1861–72.
- Noe V, Fingleton B, Jacobs K, et al. Release of an invasion promoter E-cadherin fragment by matrilysin and stromelysin-1. *J Cell Sci* 2001;114:111–8.
- Maretzky T, Reiss K, Ludwig A, et al. ADAM10 mediates E-cadherin shedding and regulates epithelial cell-cell adhesion, migration, and β -catenin translocation. *Proc Natl Acad Sci U S A* 2005;102:9182–7.
- Covington M, Burghardt R, Parrish A. Ischemia-induced cleavage of cadherins in NRK cells requires MT1-MMP (MMP-14). *Am J Physiol Renal Physiol* 2006;290:F43–51.
- Symowicz J, Adley BP, Woo MMM, Auersperg N, Hudson LG, Stack MS. Cyclooxygenase-2 functions as a mediator of lysophosphatidic acid to promote aggressive behavior in ovarian carcinoma cells. *Cancer Res* 2005;65:2234–42.
- Ghosh S, Johnson JJ, Sen R, et al. Functional relevance of urinary-type plasminogen activator- $\alpha_3\beta_1$ integrin association in proteinase regulatory pathways. *J Biol Chem* 2006;281:13021–9.
- Fridman R, Toth M, Chvyrkova I, Meroueh SO, Mobashery S. Cell surface association of matrix metalloproteinase-9 (gelatinase B). *Cancer Metastasis Rev* 2003;22:153–66.
- Niessen CM, Gumbiner BM. Cadherin-mediated cell sorting not determined by binding or adhesion specificity. *J Cell Biol* 2002;156:389–99.
- Marques F, Fonsechi-Carvasan GA, De Angelo Andrade LAL, Botcher-Luiz F. Immunohistochemical patterns for α and β -catenin, E- and N-cadherin expression in ovarian epithelial tumors. *Gynecol Oncol* 2004;94:16–24.
- Chan A, Chu KM, Lam SK, et al. Early prediction of tumor recurrence after curative resection of gastric carcinoma by measuring soluble E-cadherin. *Cancer* 2005;104:740–6.
- Syrigos KN, Harrington KJ, Karayiannakis AJ, Baibas N, Katirtzoglou N, Roussou P. Circulating soluble E-cadherin levels are of prognostic significance in patients with multiple myeloma. *Anticancer Res* 2004;24:2027–31.
- Billion K, Ibrahim H, Mauch C, Niessen CM. Increased soluble E-cadherin in melanoma patients. *Skin Pharmacol Physiol* 2006;19:65–70.
- Irby RA, Yeatman TJ. Increased Src activity disrupts cadherin/catenin-mediated homotypic adhesion in human colon cancer and transformed rodent cells. *Cancer Res* 2002;62:2669–74.
- Avizienyte E, Wyke A, Jones R, et al. Src-induced deregulation of E-cadherin in colon cancer cells requires integrin signaling. *Nat Cell Biol* 2002;4:632–38.
- DeClerck YA. Interactions between tumour cells and stromal cells and proteolytic modification of the extracellular matrix by metalloproteinases in cancer. *Eur J Cancer* 2000;36:1258–68.
- Huang LW, Garrett AP, Bell DA, Welch WR, Berkowitz RS, Mok SC. Differential expression of matrix metalloproteinase-9 and tissue inhibitor of metalloproteinase-1 protein and mRNA in epithelial ovarian tumors. *Gynecol Oncol* 2000;77:369–76.
- Davidson B, Goldberg I, Gotlieb W, et al. High levels of MMP2, MMP9, MT1-MMP, and TIMP-2 mRNA correlate with poor survival in ovarian carcinoma. *Clin Exp Metastasis* 1999;17:799–808.
- Naylor MS, Stamp GW, Davies BD, Balkwill FR. Expression and activity of MMPs and their regulators in ovarian cancer. *Int J Cancer* 1994;58:50–6.
- Zhu GG, Risteli J, Puistola U, Kauppila A, Risteli L. Progressive ovarian carcinoma induces synthesis of type I, type III, procollagens in the tumor tissue and peritoneal cavity. *Cancer Res* 1993;53:5028–32.
- McCawley LJ, Matrisian LM. Tumor progression: defining the soil around the tumor seed. *Curr Biol* 2001;11:R25–7.
- Martin J, Yung S, Robson RL, Steadman R, Davies M. Production and regulation of matrix metalloproteinases and their inhibitors by human peritoneal mesothelial cells. *Perit Dial Int* 2000;20:524–33.
- Coussens L, Tinkle C, Hanahan D, Werb Z. MMP-9 supplied by bone marrow-derived cells contributes to skin carcinogenesis. *Cell* 2000;103:481–90.
- Huang S, Van Arsdall M, Tedjarati S, et al. Contributions of stromal metalloproteinase-9 to angiogenesis and growth of human ovarian carcinoma in mice. *J Natl Cancer Inst* 2002;94:1134–42.
- Ozalp S, Tanir HM, Yalcin OT, Kabukuoglu S, Oner U, Uray M. Prognostic value of matrix metalloproteinase-9 (gelatinase-B) expression in epithelial ovarian tumors. *Eur J Gynaecol Oncol* 2003;24:417–20.
- Kamat AA, Fletcher M, Gruman LM, et al. The clinical relevance of stromal matrix metalloproteinase expression in ovarian cancer. *Clin Cancer Res* 2006;12:1707–14.
- Lengyel E, Schmalfeldt B, Konik E, et al. Expression of latent matrix metalloproteinase 9 (MMP9) predicts survival in advanced ovarian cancer. *Gynecol Oncol* 2001;82:291–8.
- Fishman DA, Bafetti LM, Banionis S, Kearns AS, Chilukuri K, Stack MS. Production of extracellular

- matrix-degrading proteinases by primary cultures of human epithelial ovarian carcinoma cells. *Cancer* 1997; 80:1457-63.
45. Demeter A, Sziller I, Csapo Z, et al. Molecular prognostic markers in recurrent and in non-recurrent epithelial ovarian cancer. *Anticancer Res* 2005;25: 2885-9.
46. Guo W, Giancotti FG. Integrin signalling during tumour progression. *Nat Rev Mol Cell Biol* 2004;5: 816-26.
47. Arias-Salgado E, Lizano S, Sarkar S, Brugge JS, Ginsberg MH, Shattil SJ. Src kinase activation by direct interaction with the integrin β cytoplasmic domain. *Proc Natl Acad Sci U S A* 2003;100:13298-302.
48. Ellerbroek SM, Halbleib JM, Benavidez M, et al. Phosphatidylinositol 3-kinase activity in epidermal growth factor-stimulated matrix metalloproteinase-9 production and cell surface association. *Cancer Res* 2001;61:1855-61.
49. Rathi A, Virmani AK, Schorge JO, et al. Methylation profiles of sporadic ovarian tumors and nonmalignant ovaries from high risk women. *Clin Cancer Res* 2002;8: 3324-31.
50. Makarla P, Saboorian MH, Ashfaq R, et al. Promoter hypermethylation profile of ovarian epithelial neoplasms. *Clin Cancer Res* 2005;11:5365-9.
51. Dwivedi DJ, Pino G, Banh A, et al. Matrix metalloproteinase inhibitors suppress transforming growth factor- β -induced subcapsular cataract formation. *Am J Pathol* 2006;168:69-79.
52. Wheelock MJ, Buck CA, Bechtol KB, Damsky CH. Soluble 80-kd fragment of cell-CAM 120/80 disrupts cell-cell adhesion. *J Cell Biochem* 1987;34:187-202.
53. Nawrocki-Raby B, Gilles C, Polette M, et al. Upregulation of MMPs by soluble E-cadherin in human lung tumor cells. *Int J Cancer* 2003;105:790-5.
54. Chunthapong J, Seftor E, Khalkhali-Ellis Z, et al. Dual roles of E-cadherin in prostate cancer invasion. *J Cell Biochem* 2004;91:649-61.
55. Liu WF, Nelson CM, Pirone DM, Chen CS. E-cadherin engagement stimulates proliferation via Rac1. *J Cell Biol* 2006;173:431-41.